

COMPOSITION AND TEMPERATURE MONITORING OF MOLTEN METAL BY A COMBINED LIBS-IR THERMOMETRY SYSTEM

Zeng Qiang, Pan Congyuan^{*}, Fei Teng, Ding Xiaokang, Wang Shengbo, Wang Qiuping^{*}

University of Science and Technology of China, Hefei, Anhui, China; e-mail: qiuping@ustc.edu.cn

The composition and temperature of molten metal in a furnace are important parameters in metallurgical industrial processing. Laser-induced breakdown spectroscopy (LIBS) is a promising technique for the in-situ quantitative composition analysis of molten metal, and infrared radiation from molten metal can be used for temperature measurement. A near-infrared spectrometer was added to a LIBS system in this work. The LIBS signal and temperature information were recorded by the same optical system and optical fiber, and the temperature and the elemental content of the molten metal could be measured simultaneously. Molten carbon steel was used to verify the system performance. The measured temperature exhibited a good consistency with the temperature that was obtained by using a commercial pyrometer, with a relative root mean square error of 0.95%. The relative standard errors of Cr and Mn composition detection were lower than 10%. These results prove that it is possible to monitor composition and temperature in a molten metal process by a LIBS systems imultaneously.

Keywords: laser-induced breakdown spectroscopy, infrared thermometry, composition, temperature, metallurgy.

МОНИТОРИНГ СОСТАВА И ТЕМПЕРАТУРЫ РАСПЛАВЛЕННОГО МЕТАЛЛА КОМБИНИРОВАННЫМ МЕТОДОМ ЛАЗЕРНО-ИСКРОВОЙ ЭМИССИОННОЙ СПЕКТРОСКОПИИ И ИК ТЕРМОМЕТРИИ

Q. Zeng, C. Pan^{*}, T. Fei, X. Ding, S. Wang, Q. Wang^{*}

УДК 543.42:669

Китайский научный технологический университет,
Хэфэй, Аньхой, Китай; e-mail: qiuping@ustc.edu.cn

(Поступила 5 июня 2017)

Для количественного анализа состава расплавленного металла в печи использован метод лазерно-искровой эмиссионной спектроскопии (LIBS), а ИК излучение расплавленного металла – для измерения температуры. Для этого в систему LIBS добавлен ИК спектрометр. Информация о сигналах LIBS и температуре регистрировалась одной и той же оптической системой и оптическим волокном. Таким образом температуру и элементное содержание расплавленного металла можно измерять одновременно. Для проверки производительности системы использована расплавленная углеродистая сталь. Измеренная температура хорошо соответствует полученной с использованием коммерческого пирометра (относительная среднеквадратическая погрешность достигала 0.95%). Относительные ошибки обнаружения Cr и Mn <10%. Полученные результаты подтверждают возможность одновременного мониторинга состава и температуры в процессе получения расплавленного металла системами LIBS.

Ключевые слова: лазерно-искровая эмиссионная спектроскопия, инфракрасная термометрия, состав, температура, металлургия.

Introduction. Composition and temperature are the most essential parameters for process control in the metallurgical industry [1–3]. With merits of rapid analysis, remote measurement, and minimal or no requirement for sample preparation, laser-induced breakdown spectroscopy (LIBS) has attracted remarkable interest for *in situ* and online quantitative analysis in metallurgy [4–7]. Infrared (IR) thermometry is a non-contact temperature-measuring method that is suitable for continuous online measurement. Many types of non-contact thermometers, such as IR thermometers, IR thermal TVs, and IR thermal imagers, have been developed [8–10].

A combination of different online measurement techniques for the direct analysis of molten metal will promote the developments in the metallurgical industry. Several works have focused on both composition and temperature measurement. Gudenau et al. [11] developed a model lance to achieve continuous elemental analysis or temperature measurement. Different detection systems were constructed with the lance to measure composition and temperature alternatively. Vanderheyden [12, 13] developed an online LIBS-based sensor to monitor the composition and temperature of the hot metal in blast-furnace runners. The experimental results of the composition measurement using LIBS were satisfactory, and the temperature was measured by a commercial pyrometer. In these studies, the temperature of the hot metal was measured by an additional commercial pyrometer or measuring system. Monfort et al. [14] established a relationship between the intensity of an optimized wavelength and the temperature by using a LIBS system. An accuracy of $\pm 15^\circ\text{C}$ was achieved, except for two outliers. However, the response efficiency of the collection system was not calibrated.

In this work, a LIBS-IR thermometry system that combines an IR spectrometer with a LIBS system was developed to monitor the temperature and elemental composition of molten steel simultaneously. The temperature was measured by an additional spectrometer in a calibrated LIBS detection system. Five carbon steel samples were smelted sequentially to test the multifunctional system in the laboratory. The metal temperature and composition were obtained simultaneously.

LIBS. The internal standard calibration method can be a reliable way to achieve quantitative analysis. Based on the Lomakin–Scheibe formula, the characteristic line intensity I can be presented by a simple equation $I = a^* C^b$. Here a is a factor that is related to the system parameters and b is the self-absorption coefficient. In general, for minor or trace elements, the self-absorption of the emission lines can be neglected. Thus, factor b is approximately equal to 1, and the intensity and the concentration are linearly related. For LIBS analysis, the content of reference element can be regarded as a constant. Therefore, the intensity ratio is directly proportional to the concentration of the analytical element, which can be presented by the equation:

$$R = I_x/I_{\text{ref}} = a_1 C_x/a_2 C_{\text{ref}} = AC_x. \quad (1)$$

Here I_x represents the spectral line intensity of the analytical element, C_x is the concentration of analytical element, I_{ref} is the intensity of the reference spectral line, C_{ref} is the concentration of reference element, and A , a_1 , and a_2 are constants that are determined by the experimental system.

For analytical elements with a wide concentration range, quadratic or higher polynomial models should be used to correct the effect that is caused by a high concentration. The internal standard calibration model can be presented as

$$R = I_x/I_{\text{ref}} = A_0 + A_1 C_x + A_2 C_x^2 + \dots \approx A_0 + A_1 C_x. \quad (2)$$

For convenience, it is feasible to take the first two terms of the polynomial to construct the calibration model.

The process of internal standard calibration is routine. First, the LIBS spectra of a series of standard samples are obtained at different delay times. Second, the spectral backgrounds are corrected, and the peaks are identified. Third, possible spectral characteristic lines are confirmed by referring to the atomic spectra database. Fourth, the calibration model of each characteristic line is constructed individually, and the chosen characteristic line is saved as an analysis line, based on an estimation of the calibration model [15]. Calibration models can be obtained with the multi-line internal standard calibration (MLISC) method [16]. Finally, the concentration of the analyzed element can be calculated by using the constructed calibration model.

IR thermometry. In 1900, Planck established the distribution of the radiant exitance $M_{b\lambda}$ ($\text{W}/\text{m}^2 \cdot \mu\text{m}^{-1}$) of a blackbody at different temperatures according to quantum statistical theory. This principle, which is termed Planck's law, is expressed as follows:

$$M_{b\lambda} = C_1/(\lambda^{-5}[\exp(C_2/\lambda T) - 1]), \quad (3)$$

with Wien's approximation

$$M_{b\lambda} = C_1/(\lambda^5 \exp(C_2/\lambda T)), \quad (4)$$

where λ is the radiation wavelength, and T is the thermodynamic temperature of the body. The first Planck constant C_1 is $2\pi hc^2$, and the second Planck constant C_2 is hc/k , h is the Planck constant, c is the speed of light, and k is the Boltzmann constant.

According to Planck's law, the thermodynamic temperature of a body can be deduced from the IR spectrum through total radiation, brightness (i.e., radiation of a narrow waveband), or multispectral radiation thermometry [17]. Double-wavelength thermometry as the simplest mode of multispectral radiation thermometry can reduce the influence of emissivity on temperature measurement considerably. The thermodynamic temperature is deduced from the ratio of radiant exitances of two adjacent wavelengths. The ratio R of exitances M_{λ_1} and M_{λ_2} , which correspond to wavelengths λ_1 and λ_2 , can be expressed as follows:

$$R = \frac{M_{\lambda_1}}{M_{\lambda_2}} = \frac{\varepsilon_1 C_1 \lambda_2^5 \exp(C_2/\lambda_2 T)}{\varepsilon_2 C_1 \lambda_1^5 \exp(C_2/\lambda_1 T)} = \frac{\varepsilon_1 \lambda_2^5 \exp(C_2/\lambda_2 T)}{\varepsilon_2 \lambda_1^5 \exp(C_2/\lambda_1 T)}, \quad (5)$$

where ε_1 and ε_2 are the emissivities that correspond to wavelengths λ_1 and λ_2 under temperature T . Thus, the temperature T that is obtained through double-wavelength thermometry can be expressed as

$$T = \frac{C_2(\lambda_2^{-1} - \lambda_1^{-1})}{\ln R - \ln(\varepsilon_1/\varepsilon_2) - \ln(\lambda_2^5/\lambda_1^5)} = \frac{C_2(\lambda_2^{-1} - \lambda_1^{-1})}{\ln(M_{\lambda_1}/M_{\lambda_2}) - \ln(\varepsilon_1/\varepsilon_2) - \ln(\lambda_2^5/\lambda_1^5)}. \quad (6)$$

The ratio of the collection intensity (I_λ) to the radiant exitance (M_λ) is defined as the response efficiency (η) of the collection system, and then the radiant exitance can be expressed as $M_\lambda = I_\lambda/\eta$. The collection intensities are assumed to be I_{λ_1} and I_{λ_2} , and the response efficiencies are η_1 and η_2 , which correspond to wavelengths λ_1 and λ_2 , respectively. Moreover, ε_1 can equal ε_2 when the values of λ_1 and λ_2 are close. Equation (6) can be transformed as follows:

$$T = \frac{C_2(\lambda_2^{-1} - \lambda_1^{-1})}{\ln(M_{\lambda_1}/M_{\lambda_2}) - \ln(\varepsilon_1/\varepsilon_2) - \ln(\lambda_2^5/\lambda_1^5)} = \frac{C_2(\lambda_2^{-1} - \lambda_1^{-1})}{\ln \frac{I_{\lambda_1}/\eta_1}{I_{\lambda_2}/\eta_2} - \ln(\lambda_2^5/\lambda_1^5)}. \quad (7)$$

Experimental setup. Figure 1 presents a schematic diagram of the LIBS-IR thermometry system, and the system parameters are listed in Table 1. The signal of the induced plasma is coupled into multi-furcated fiber optics via a collection lens and is then transported into spectrometer channel-1 for quantitative analysis, whereas the IR signal is transported into spectrometer channel-2 (a near IR spectrometer) for temperature measurement. The reference temperature is measured simultaneously by a commercial pyrometer.

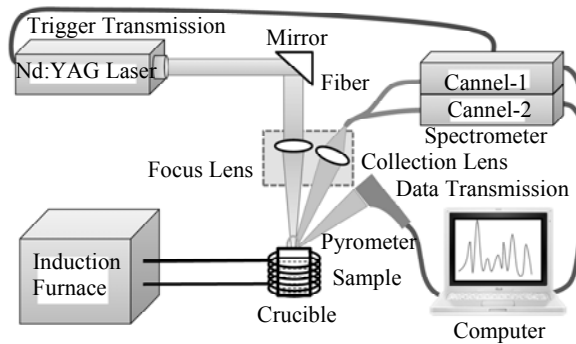


Fig. 1. Schematic diagram of the LIBS-IR thermometry system.

To obtain the original radiation intensity of the induced plasma and IR signals, the LIBS-IR thermometry system was calibrated with a standard light source (lamp F1018, certificated by the National Institute of Metrology of China) to eliminate the effect of response efficiency. Especially, the calibration of the IR thermometry module by using the corrected radiation power and the recorded spectrum of the standard light source helps restore the original radiation power (i.e., radiant exitance) of molten metal. Five carbon steel samples were melted in an induction furnace for the experiment. Their components are listed in Table 2. Each recorded LIBS spectrum is the average of five measurements with a delay time of $0.3 \mu\text{s}$, and 10 spectra were saved for subsequent analysis. The IR signal can be recorded from the beginning to the end of the smelting process, except when plasma is being generated.

TABLE 1. Parameters of the LIBS-IR Thermometry System

Nd:YAG laser	Wavelength	1064 nm	
	Pulse width	10 ns	
Spectrometer	Pulse energy	120 mJ	
	Repetition	2 Hz	
	Stability	3%	
Pyrometer	Range	Channel-1	Channel-2
	Resolution	185–310 nm	200–1100 nm
	Integration time	0.12 nm 2 ms	2.5 nm 4 ms
Induction furnace	Maximum power	900–2500°C 15 kV · A	

TABLE 2. Components of the Analyzed Samples

Sample	C	S	Si	Mn	P	Cr	Ni	Cu	Fe
1	0.31	0.031	0.48	0.87	0.051	0.28	0.12	0.355	97.503
2	0.458	0.017	0.188	0.582	0.022	0.036	0.042	0.132	98.523
3	0.512	0.01	0.352	0.69	0.022	0.077	0.06	0.154	98.123
4	0.12	0.014	0.12	0.258	0.013	0.022	0.034	0.122	99.297
5	0.183	0.011	0.241	0.459	0.0099	0.024	0.015	0.02	99.037

Results and discussion. *Composition analysis.* Before online component detection, experiments were conducted on molten carbon steels to construct quantitative calibration models. Figure 2a shows the calibration curves for Cr and Mn as constructed by the MLISC method. The chosen line pairs for Cr analysis are Cr II 288.09/Fe I 292.39, Cr II 304.08/Fe II 282.33, and Cr II 288.09/ Fe I 299.44 nm. The average relative error with leave-one-out cross validation (ARECV) and the root mean square error with leave-one-out cross validation (RMSECV) are 4.3% and 0.0037 wt.%, respectively. The chosen line pairs for Mn analysis are Mn II 279.83/Fe I 243.93, Mn II 279.83/Fe II 237.36, and Mn II 279.83/Fe I 236.86 nm. The obtained ARECV and RMSECV are 0.8% and 0.032 wt.%, respectively.

An online component analysis was performed every 60 s using the constructed calibration models. The measurement parameters were consistent with the optimized experimental parameters that were used to construct the calibration models. Figure 2b shows the online molten steels quantitative analysis results for Cr and Mn. The results indicate that the average relative standard errors of Cr and Mn are less than 10%.

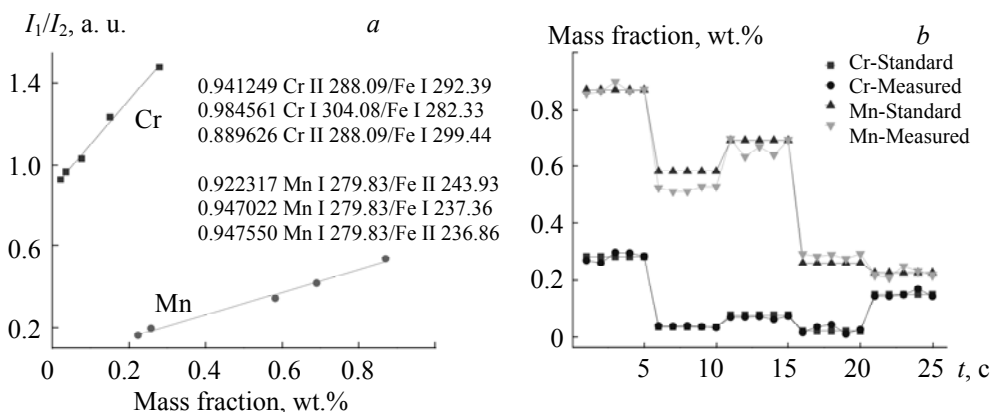


Fig. 2. Calibration curves using MLISC (a); online measurement errors of Cr and Mn (b).

Temperature measurement. A calibration of the collection system is essential for temperature measurement. Figure 3a shows the corrected radiation power of the standard light source, which is defined as $M_1(\lambda)$. Figure 3b shows the collected spectrum of the lamp via channel-2, which is defined as $I_1(\lambda)$. The response efficiency of the collection system can be expressed as $\eta(\lambda) = I_1(\lambda)/M_1(\lambda)$. The original radiation power

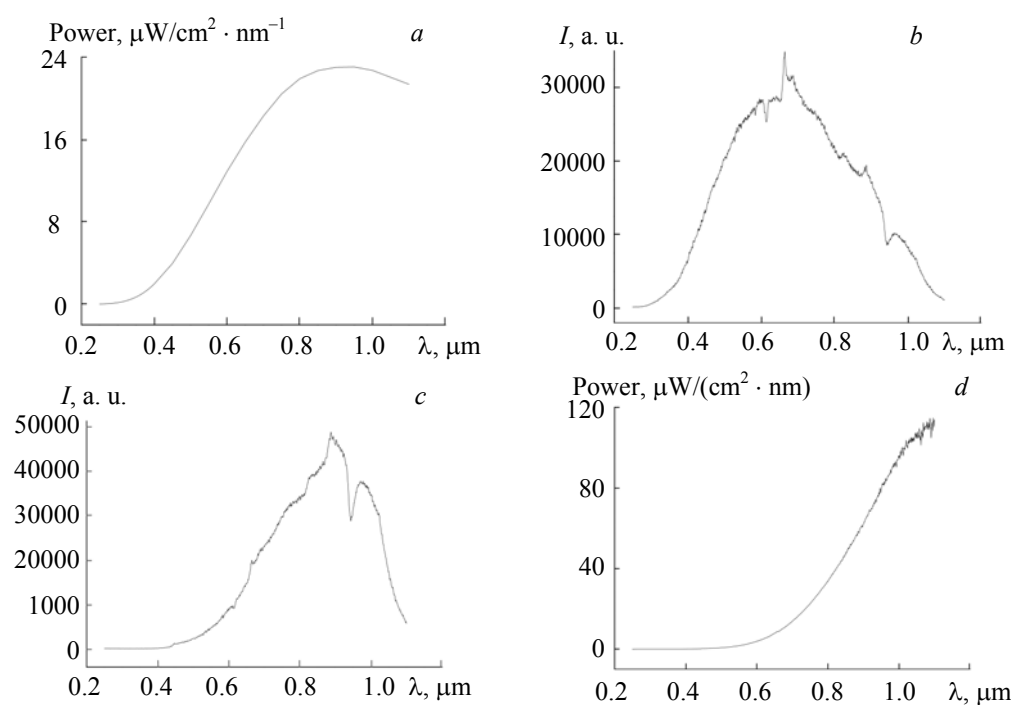


Fig. 3. Corrected radiation power (a); collected spectrum of the standard light source (b); collected spectrum of molten steel (c); radiation power of molten steel (d).

of molten steel can be deduced from the collection spectrum with the obtained response efficiency. Figure 3c shows a collection spectrum of molten steel, which is defined as $I(\lambda)$. The original radiation power of molten steel is defined as $M_2(\lambda)$, which can be calculated from the expression $M_2(\lambda) = I_2(\lambda)/\eta(\lambda) = I_2(\lambda)M_1(\lambda)/I_1(\lambda)$. As shown in Fig. 3d, the outline of the obtained original radiation power of molten steel is close to that of the radiation power of a blackbody under the same temperature. The smelting temperature can be calculated by using the obtained radiation power.

The temperature was measured every 2 s throughout the steel melting period. The smelting temperature was calculated from the intensity ratio of wavelengths 1.0 and 0.7 μm , which referred to the calculating method of the commercial pyrometer. Figure 4 compares of the changes between the calculated temperature (measured temperature) that is obtained by double-wavelength thermometry and the reference temperature that is obtained by the pyrometer from the preheating state to the molten state, and finally to the cooling state. The relative root mean square error can reach 0.95%, without considering the compensation of emissivity. Thus, the measurement accuracy is acceptable and can be improved through highly accurate alignment and measurement synchronization.

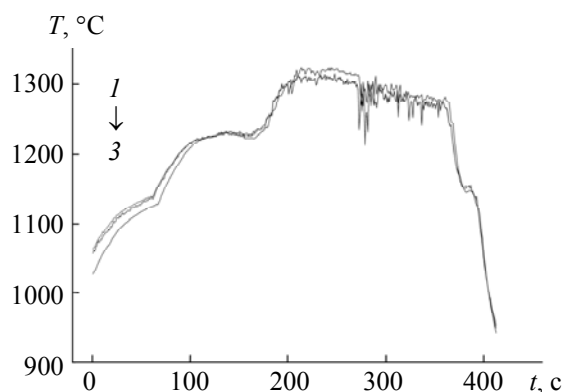


Fig. 4. Comparison of measured temperature by double-wavelength thermometry (1), by fitting the full spectra (2), and reference temperature (3).

The smelting temperature that is obtained by fitting the measured spectra of the thermal emission is also given out in Fig. 4. The difference between the measured temperature that is obtained by fitting and that which is obtained by double-wavelength thermometry is tiny. The significance of recording of the full spectra is more than the fitting for the temperature parameter. With a reasonable emissivity function, the transient emissivities at different wavelengths can be solved by using the full spectra. Furthermore, the true temperature can be calculated without approximation.

Conclusion. The temperature and composition of molten metal can be monitored simultaneously with a LIBS system. Moreover, the IR spectrum can be detected by using a spectrometer instead of a compound photodetector that is combined with filters. The use of a spectrometer to record the full spectrum within milliseconds can expand the measuring range significantly and make the calculation of transient emissivity and true temperature of the molten metal possible. The proposed multifunctional system can be applied easily to metallurgical plants by changing the lens system into a telescope system. Thus, the LIBS-IR thermometry system can monitor the composition and temperature for the molten metal process simultaneously, which can help optimize the metallurgical process control.

Acknowledgment. The authors are grateful for financial support from National Key Scientific Instrument and Equipment Development Projects of China (No. 2014YQ120351).

REFERENCES

1. M. Hatano, Y. Matoba, K. Otsuka, M. Yoshiki, T. Miyagi, *Trans. Iron Steel Inst. Jpn.*, **22**, 534–542 (1982).
2. Ü. Çamdali, M. Tunç, F. Dikeç, *Appl. Therm. Eng.*, **21**, 643–655 (2001).
3. T. P. Fredman, H. Saxen, *Metallurg. Mater. Trans. B*, **29**, 651–659 (1998).
4. A. Khalil, M. Richardson, C. Barnett, L. Johnson, *J. Appl. Spectrosc.*, **73**, 735–742 (2006).
5. R. Noll, C. Fricke-Begemann, M. Brunk, S. Connemann, C. Meinhardt, M. Scharun, V. Sturm, J. Makowe, C. Gehlen, *Spectrochim. Acta B: At. Spectrosc.*, **93**, 41–51 (2014).
6. L. Peter, V. Sturm, R. Noll, *Appl. Opt.*, **42**, 6199–6204 (2003).
7. N. Ramaseder, J. Gruber, J. Heitz, D. Baeuerle, W. Meyer, J. Hochoertler, *Metall. Ital.*, **2**, 60–63 (2004).
8. A. Rogalski, K. Chrzanowski, *Metrol. Meas. Syst.*, **21**, 565–618 (2014).
9. A. Rogalski, *Opto-Electron. Rev.*, **20**, 279–308 (2012).
10. B. Müller, U. Renz, *Rev. Sci. Instrum.*, **72**, 3366–3374 (2001).
11. H. W. Gudenau, K. T. Mavrommatis, L. Ernenputsch, *Stahl Eisen*, **121**, 45–50 (2001).
12. G. Mathy, G. Monfort, B. Vanderheyden, V. Tusset, *Metall. Anal.*, **31**, 21–23 (2011).
13. G. Monfort, L. Bellavia, B. Vanderheyden, V. Tusset, *Metall. Anal.*, **32**, 6–11 (2012).
14. G. Monfort, L. Bellavia, M. Tonteling, C. Ojeda, O. Ansseau, *J. Appl. Laser Spectrosc.*, **1**, 1–6 (2014).
15. C. Aragon, J. A. Aguilera, F. Penalba, *Appl. Spectrosc.*, **53**, 1259–1267 (1999).
16. C. Pan, X. Du, N. An, Q. Zeng, S. Wang, Q. Wang, *Appl. Spectrosc.*, **70**, 702–708 (2016).
17. M. Fuchs, C. B. Tanner, *Agron. J.*, **58**, 597–601 (1966).